ORNL
MASTER COPY

ORNL 1604
Engineering

UNSTEADY STATE FLOW OF STEAM FROM A HIGH PRESSURE SYSTEM

W. S. Brown

OAK RIDGE NATIONAL LABORATORY
OPERATED BY
CARBIDE AND CARBON CHEMICALS COMPANY
A DIVISION OF UNION CARBIDE AND CARBON CORPORATION
UCC
POST OFFICE BOX P
OAK RIDGE, TENNESSEE

ORNL-1604

Copy No. 12

Contract No. W-7405-eng-26

REACTOR EXPERIMENTAL ENGINEERING DIVISION

UNSTEADY STATE FLOW OF STEAM FROM A HIGH PRESSURE SYSTEM

Wayne S. Brown

DATE ISSUED

NOV 24 1953

OAK RIDGE NATIONAL LABORATORY
Operated by
CARBIDE AND CARBON CHEMICALS COMPANY
A Division of Union Carbide and Carbon Corporation
Post Office Box P
Oak Ridge, Tennessee

ORNL 1604
Engineering

INTERNAL DISTRIBUTION

1. C. E. Center
2. Biology Library
3. Health Physics Library
4-5. Central Research Library
6. Reactor Experimental Engineering Library
7-11. Laboratory Records Department
12. Laboratory Records, ORNL RC
13. C. E. Larson
14. W. B. Humes (K-25)
15. L. B. Emlet (Y-12)
16. A. M. Weinberg
17. E. H. Taylor
18. E. D. Shipley
19. C. E. Winters
20. F. C. VonderLage
21. R. C. Briant
22. J. A. Swartout
23. S. C. Lind
24. F. L. Culler
25. A. H. Snell
26. A. Hollaender
27. M. T. Kelley
28. W. J. Fretague
29. G. H. Clewett
30. K. Z. Morgan
31. T. A. Lincoln
32. A. S. Householder
33. C. S. Harrill
34. D. S. Billington
35. D. W. Cardwell
36. E. M. King
37. R. N. Lyon
38. J. A. Lane
39. A. J. Miller
40. R. B. Briggs
41. A. S. Kitzes
42. O. Sisman
43. R. W. Stoughton
44. C. B. Graham
45. W. R. Gall
46. H. F. Poppendiek
47. S. E. Beall
48. J. P. Gill
49. D. D. Cowen
50. W. M. Breazeale (consultant)
51. R. A. Charpie
52. G. C. Williams
53. P. C. Zmola
54. P. R. Kasten
55. R. J. Goldstein
56. D. G. Thomas
57. M. Richardson
58. H. A. MacColl
59. C. G. Lawson
60. D. G. Davis
61. D. C. Hamilton
62. R. H. Chapman
63. M. J. Skinner
64. W. D. Allred

EXTERNAL DISTRIBUTION

65-79. W. S. Brown, University of Utah
80. J. F. Bailey, University of Tennessee
81. P. Pasqua, University of Tennessee
82. R. V. Bailey, Tulane University
83. J. I. Lang, Armour Research Foundation
84. R. F. Bacher, California Institute of Technology
85. D. B. Benedict, C&CCC, South Charleston
86-329. Given distribution as shown in TID-4500 under Engineering Category

DISTRIBUTION PAGE TO BE REMOVED IF REPORT IS GIVEN PUBLIC DISTRIBUTION

TABLE OF CONTENTS

CHAPTER		PAGE
I.	GENERAL INTRODUCTION	1
	Introduction	1
	Literature Survey	3
II.	EXPERIMENTAL EQUIPMENT	4
	Description of Apparatus	4
	Operation	8
III.	ANALYTICAL TREATMENT OF THE PROBLEM	11
	Theoretical Considerations	11
	Analytical Treatment	12
	Coefficient of Discharge	17
IV.	EXPERIMENTAL RESULTS	26
	Analysis of Temperature Data	26
	Pressure Drop versus Time	37
	Flow Rates	40
	Heat Release Rates	48
V.	CONCLUSIONS AND RECOMMENDATIONS	49
BIBLIOGRAPHY		51
APPENDIX		53

LIST OF TABLES

TABLE		PAGE
I.	Tabulated Calculations	19
II.	Tabulated Calculations	20
III.	Tabulated Calculations	21
IV.	Results of Calculations	22
V.	Results of Calculations	23
VI.	Results of Calculations	24
VII.	Power Density Attained with Corresponding Pressure and Vapor Fraction	38
VIII.	Comparison of Flow Rates Obtained Using Grashof Equation and the Analytical Method	45

LIST OF FIGURES

FIGURE		PAGE
1.	Pressure Vessel with Thermocouple Locations	5
2.	Details of Upper Section of Vessel	6
3.	Photograph of Apparatus Ready for Testing	9
4.	Location of Pertinent State Points on T-S Diagram with Corresponding Physical Locations in Vessel	14
5.	Pressure vs. Quality Diagram with Lines of Constant Internal Energy and Constant Specific Volume	18
6.	Complete Test Data from Run 2A	27
7.	Complete Test Data from Run 1A	28
8.	Complete Test Data from Run 4A	29
9.	Temperature Data from Run 4A Plotted on Mollier Chart	34
10.	Temperature Data from Run 1A Plotted on Mollier Chart	35
11.	Variation of Pressure with Time for Various Initial Weights of Liquid	39
12.	Variation of Pressure with Time as Computed and as Measured in Run 2A	41
13.	Variation of Pressure with Time as Computed and as Measured in Run 1A	42
14.	Variation of Pressure with Time as Computed and as Measured in Run 4A	43
15.	Variation of Weight of Liquid in Vessel with Time as Computed and as Measured in Runs 2A, 1A, and 4A	46

CHAPTER I

GENERAL INTRODUCTION

Introduction

The purpose of this presentation is to determine how much heat may be removed from a boiling liquid in the form of vapor, and how much liquid is entrained in the vapor as a result of the high heat release rates. This problem has important applications in industry.

It is common practice in industry to protect chemical reactors, boilers, refrigeration systems, etc., with safety devices such as pressure relief valves and rupture discs. If a reaction gets out of control the vapor pressure of one of the constituents may rise until the pressure vessel is damaged, if no means of reducing the pressure is available. The function of the pressure relief device is to vent the system to a lower pressure region and allow vapor to leave the vessel.

As vapor leaves the liquid surface, it may entrain sufficient quantities of liquid to choke off the pressure relief device and prevent a rapid decrease in pressure. At the same time the reaction may proceed at a rate such that more vapor is formed than leaves through the venting device resulting in a further increase in pressure.

The problem then arises, how much heat may be removed from a liquid surface in the form of vapor, and how much liquid will be entrained in the vapor for a given heat release rate. The term heat release rate as used here is defined as the product of the vapor flow

rate, expressed as pounds per sec per sq ft of surface, and the latent heat of the liquid expressed in Btu per lb, and has the units Btu per sec per sq ft.

A modest experiment was performed using water as the fluid. To achieve high heat release rates a closed vessel containing saturated liquid and saturated vapor at high pressure was vented to the atmosphere through a restricting tube. The most difficult problem in determining the heat release rate was finding the flow rate. The rate of change in pressure and hence the flow rate for a container of a given volume is dependent on the original pressure, the cross sectional area of the restricting tube and the amount of liquid initially in the vessel. In this investigation all three of these conditions were varied.

From an analytical method presented in this report the flow rate and rate of pressure change could be predicted. By comparing the predicted rates with measurements of the same quantities the validity of the analytical method was determined. Temperature measurements were made to determine the condition of the vapor leaving the system and the approximate location of the boiling level.

Tests were made at initial pressures of 1540 psia and 540 psia and with initial liquid weights of two, four and six pounds. Two restricting tubes were used in different tests. The tubes were one eighth of an inch long with diameters of 0.0625 in and 0.0938 in. The system pressure, the weight of liquid in the vessel, and pertinent temperatures were recorded during the time the pressure was decreasing.

The heat release rates varied throughout the test run. The highest heat release rate obtained was 758 Btu per sec per sq ft.

While the primary purpose of the tests was to obtain information on attainable heat release rates and liquid entrainment, the flow rates obtained and the rate of pressure change for an unsteady state system of this type are of interest. Since the rate of heat release from the system is dependent on the flow rate and rate of pressure change, all three of these items will be discussed in this presentation.

Literature Survey

Very little literature exists which has a direct bearing on the problem. Jacob (1) treats the mechanism of boiling and reports results of experimental work in boiling studies. The main aim of his work was to find basic data on boiling and boiling heat transfer, and he did not attempt to study the problem of removing energy from a boiling liquid in the form of vapor. Kennan (2) briefly treats the unsteady state system of the type used in this experiment and gives a general flow equation for such a system. Benjamin and Miller (3) present results of an investigation of the flow of a flashing mixture of water and steam in pipes. This is a somewhat different problem, but is related to the experiment in that both involve the flashing of liquid to steam as a result of a decrease in pressure.

---

(1) Numbers in parentheses refer to similarly numbered references in bibliography at end of paper.

CHAPTER II

DESCRIPTION OF EXPERIMENTAL EQUIPMENT

Description of Apparatus

The pressure vessel was constructed from four inch schedule 80, type 347 stainless steel pipe. The vessel was designed to operate at pressures up to 2000 psia and was tested hydrostatically at a pressure of 3000 psia. Stainless steel was used as a construction material to make possible the use of corrosive solutions in tests following the tests made with water. Figure 1 is a sketch of the vessel showing details of construction. The flanges hold a rupture disc which serves as the primary pressure relief device. A pressure connection and a thermocouple inlet are provided in the vessel and another thermocouple is located downstream from the restricting tube in the lower flange. The tube is held in place by a recessed head cap screw with an axial hole to permit steam passage. The region above the retaining bolt is packed with one quarter inch ceramic Berl saddles, of the type commonly used in packing chemical process columns, to distribute the flow across the entire enlarged area and thereby decrease the velocity of the flowing steam. The ceramic saddles are contained in a screen basket held in place by the thermocouple radiation shield and the associated retaining ring. Figure 2 shows details of the upper section of the vessel.

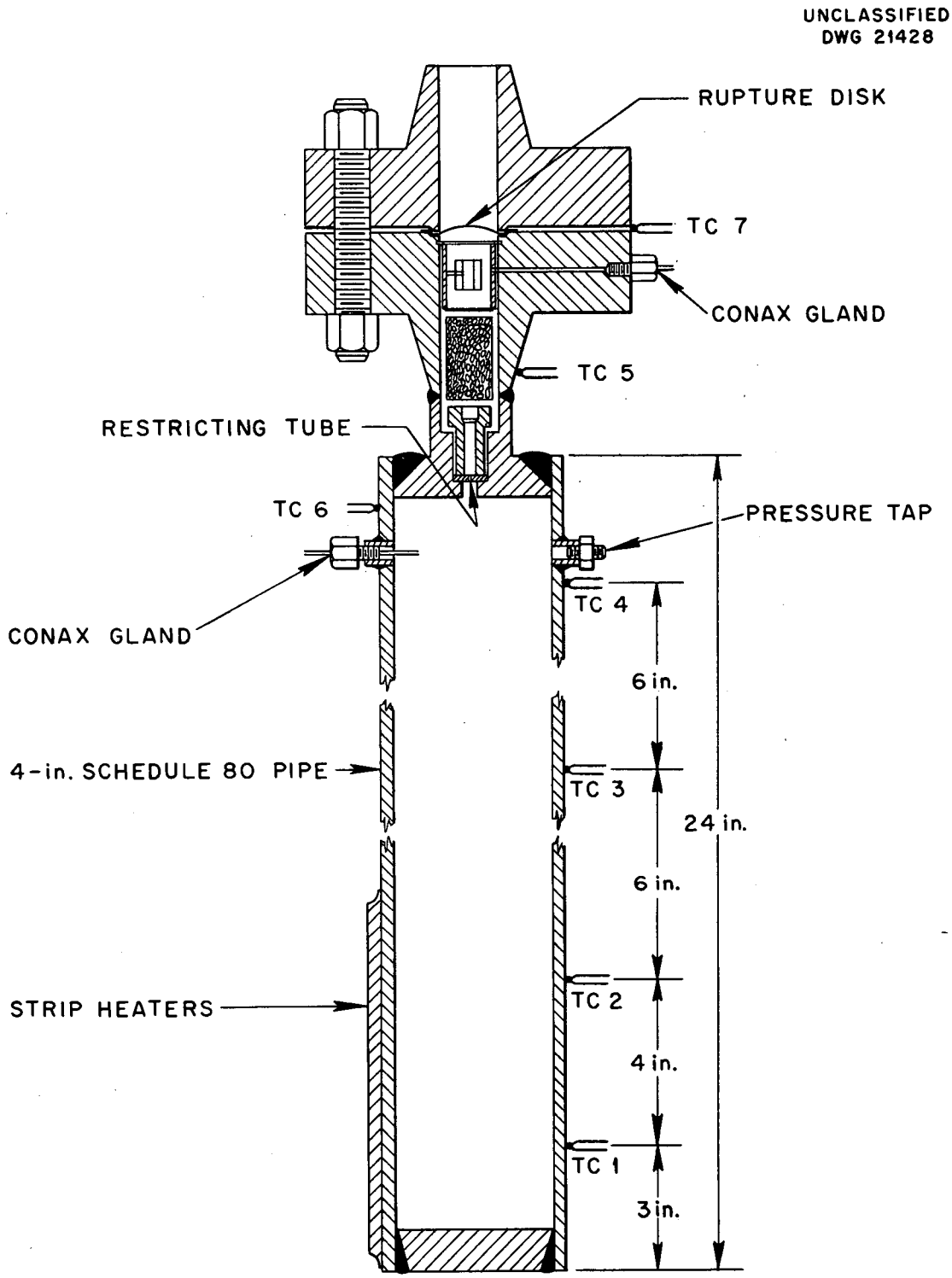

Fig. 1. Pressure Vessel with Thermocouple Locations.

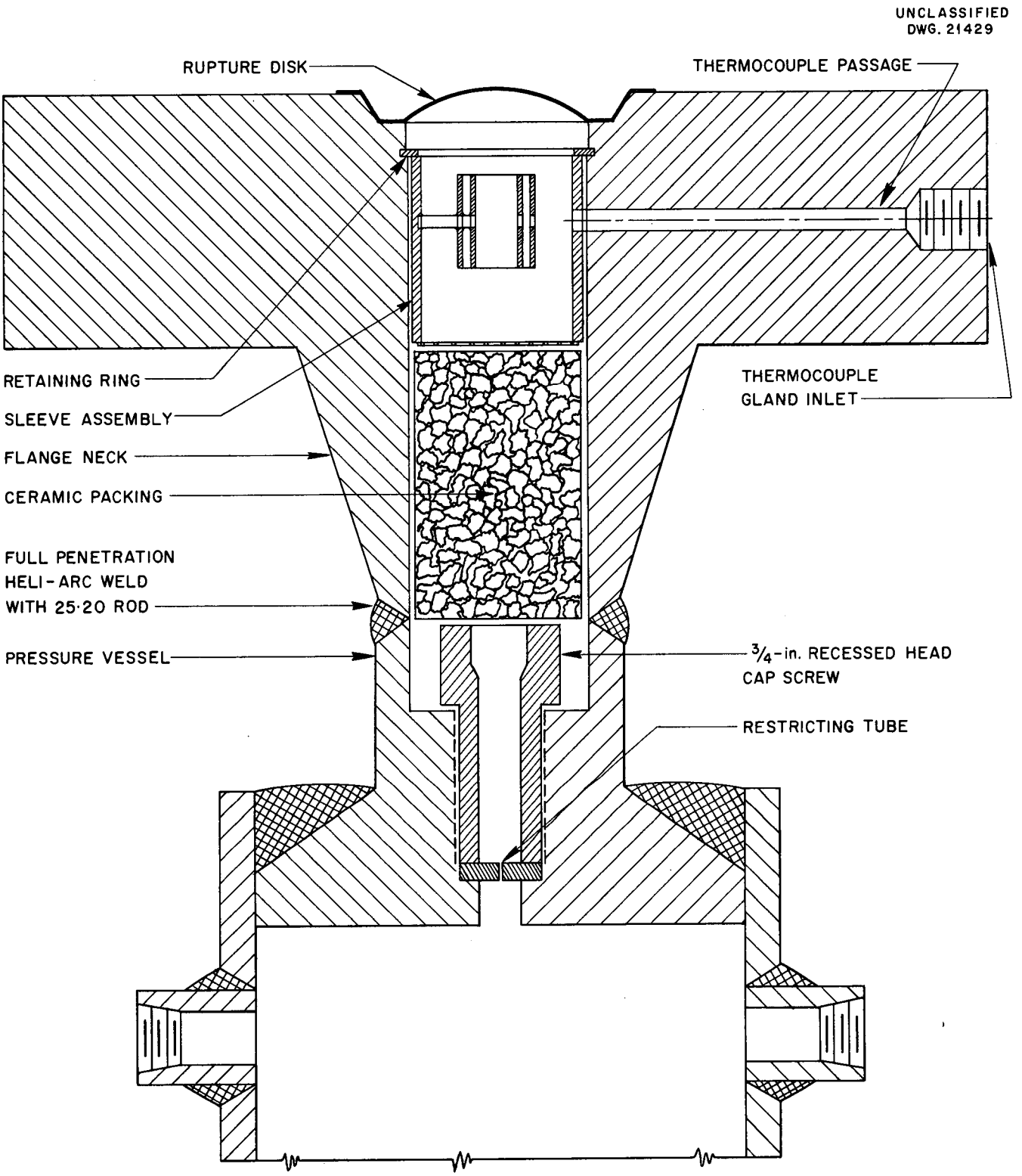

Fig. 2. Details of Upper Section of Vessel.

The two thermocouples entering the pressure vessel were constructed from 30 gage (0.010 in diameter) iron-constantan wire with a very small welded head at the junction. Conax pressure seal glands were used to introduce the thermocouples into the pressure system. The Conax gland uses powdered talc as a sealant and permits the use of a bare wire thermocouple rather than a thermocouple in a well. This is desirable since fast response is desired. Five other thermocouples were welded to various points on the outside of the vessel.

The pressure was measured with a Baldwin strain gage-type pressure cell.

A weigh mechanism was constructed to record the weight of the liquid and vapor in the vessel during the test run and thereby give an indication of the flow rate as a function of time. The deflection of a three-quarter inch square, steel, cantilever beam, on which the entire vessel was supported, was measured with a Shevitz microformer. The deflection of the beam was proportional to the weight of the test assembly. The signal from the microformer was recorded on an electronic recorder. Four pounds of liquid in the vessel caused full scale deflection on the recorder. Under static conditions a calibration indicated that the accuracy was within three per cent. Two different baffle arrangements were used to eliminate the error due to the thrust produced by the steam leaving the vessel. It was concluded that the thrust from steam leaving was not a large source of error.

All of the measurements made during the test were recorded on electronic strip-chart recorders. A more complete description of the instruments is given in the appendix.

The vessel was heated with strip heaters located around the circumference of the lower ten inches of the vessel and with a calrod heater around the neck of the flange to prevent condensation in this region. The vessel was insulated with a two inch layer of magnesia insulating material.

Figure 3 is a photograph of the vessel supported on the weigh beam ready for a test run.

Operation

In operation the vessel was filled to the desired level with a known amount of water, assembled, and supported on the weigh beam. The heaters were turned on and the temperatures were closely observed. It was desirable to have the region above the tube hotter than the rest of the system to prevent condensation in this region. The pressure tap line was opened to vent air from the system and closed when steam began to pass through it. At this point a final calibration was made on the weigh mechanism.

When the system pressure neared the burst pressure for the rupture disc, the power was decreased to allow the system to approach equilibrium before the burst. When the pressure in the bomb became sufficiently high the rupture disc burst and the steam passed through

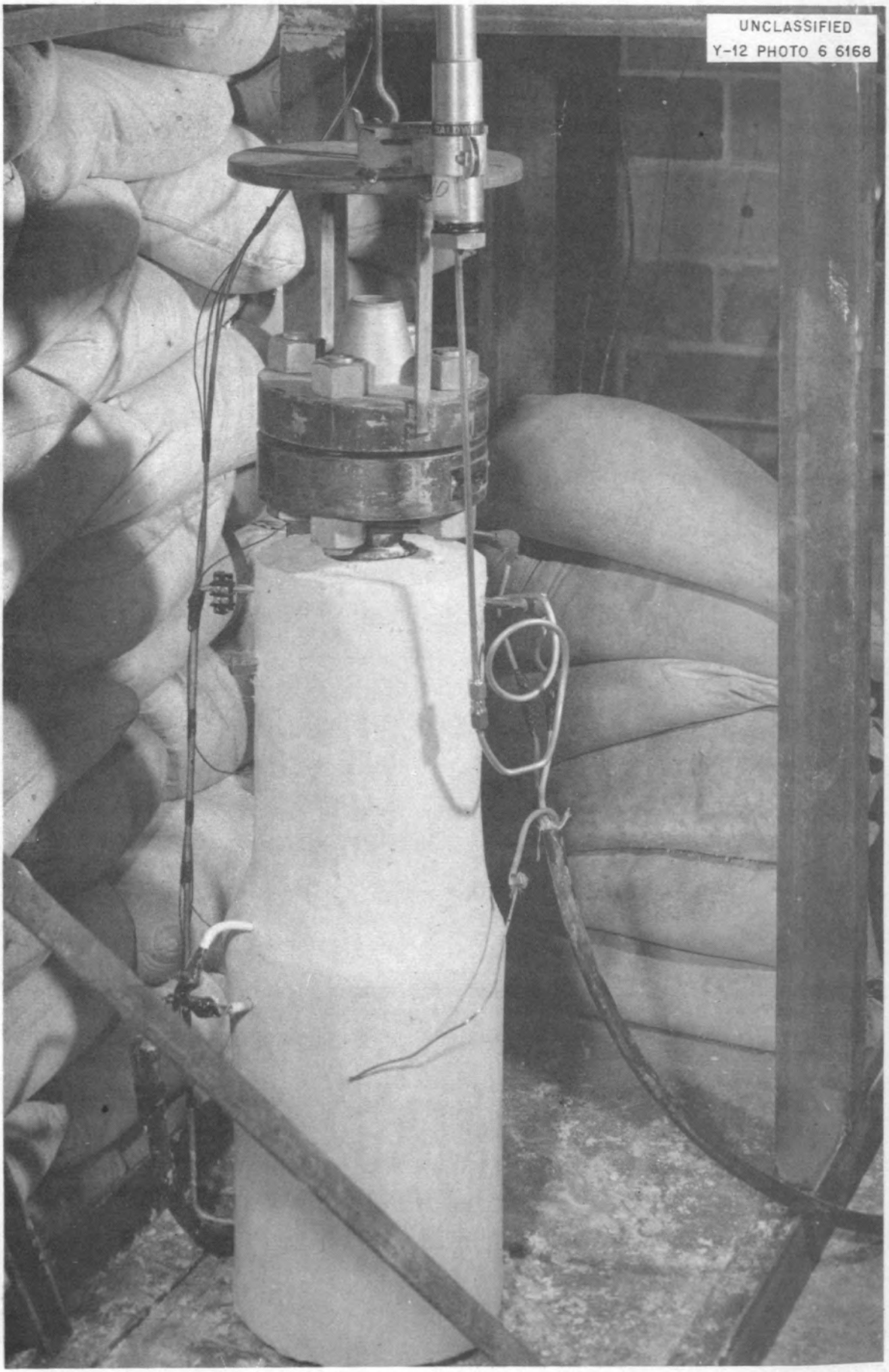

Fig. 3. Photograph of Apparatus Ready for Testing.

the tube and out of bomb to the atmosphere. The steam flow continued as long as water was being vaporized in the vessel.

The data obtained during the test run were pressure in the vessel, steam temperature in the vessel, steam temperature downstream from the restricting tube, five temperatures at various points on the vessel, and the weight of material in the vessel. The five temperatures on the vessel wall and the steam temperature in the vessel were recorded on a multipoint recorder. The downstream temperature, pressure, and weight were recorded on single pen recorders.

CHAPTER III

ANALYTICAL TREATMENT OF THE PROBLEM

Theoretical Considerations

Saturated liquid in a container at high pressure has a higher internal energy than saturated liquid at atmospheric pressure. If the pressure is lowered by some means, such as venting the vessel to the atmosphere, the liquid tends to reach a lower internal energy corresponding to saturation conditions at the lower pressure. The difference in energy between these two states is available to provide the necessary latent heat to vaporize a portion of the liquid.

The mechanism of energy release due to rapid pressure reduction in such a system may be described by a series of steps as follows. Consider an adiabatic system in which at a given time, t_1, there exists a mass of saturated liquid, m_{f1}, and a mass of saturated vapor, m_{g1}, in the vessel at pressure, p_1. As the system is vented a portion of the vapor, Δm_{g1}, leaves the vessel. There remains in the vessel a liquid mass, m_{f1}, and a vapor mass, $m_{g1} - \Delta m_{g1}$. For the constant volume system the loss in vapor is accompanied by a decrease in pressure to a new pressure, p_2. The difference in the internal energy of the saturated liquid between states 1 and 2 is available to vaporize part of the liquid, m_{fg1}. At time, t_2, the system then contains a mass of liquid, $m_{f2} = m_{f1} - m_{fg1}$, and a mass of vapor, $m_{g2} = m_{g1} - \Delta m_{g1} + m_{fg1}$ at pressure p_2. The process is then repeated. The energy release of

course takes place continuously, but may conveniently be thought of as being a series of discrete steps. The process will continue until the pressure in the vessel is equal to the outside pressure.

In the tests liquid was evaporated after the pressure reached atmospheric pressure due to heat transferred to the liquid from the walls of the vessel.

Analytical Treatment

The rate of pressure change in the vessel, the vapor flow rate, and the heat release rate may be computed for the system by an analytical treatment, if the restricting tube area, the initial weight of liquid in the vessel, and the initial pressure are known. The following assumptions are made.

1. No heat is transferred into the liquid and vapor after the pressure is released.
2. The flow across the restricting tube is based on an isentropic expansion.
3. The flow process is accurately represented by a series of flow processes for short time intervals over which conditions remain constant.
4. Critical flow is obtained through the restricting tube, and the downstream pressure is equal to 0.575 times the upstream pressure.
5. The vapor entering the restricting tube is saturated. (Wet or superheated conditions may be assumed if desirable.)

6. The unsteady state flow across the restricting tube may be approximated by a steady state equation.

Figures 4(a) and 4(b) are helpful in presenting the method of computation. In Figure 4(a) the state points of the liquid and vapor are located on a temperature-entropy diagram. Points a and b are respectively the state points for the liquid and vapor in the vessel. Point a' is the state of the liquid plus the vapor in the vessel. Point c is the state of the vapor at the critical flow pressure as it leaves the vessel. The numerical subscripts represent time. Figure 4(b) indicates the physical location of the points a, b, and c on a schematic sketch of the vessel.

The transfer of mass from the vessel to the atmosphere is an unsteady state process and may be represented by the equation

$$M_1u_1 = M_2u_2 + \int_1^2 (h_c + KE_c)dm, \tag{1}$$

where M is the mass of the liquid plus vapor in the vessel, u is the internal energy of the liquid plus vapor in the vessel, h_c is the enthalpy of the vapor at point c, KE_c is the kinetic energy of the vapor at point c, dm is the instantaneous mass of the vapor leaving the vessel, and the numerical subscripts denote time at the beginning and the end of the time interval. By assuming that conditions remain constant over short time intervals (1) may be written as

$$M_1u_1 = M_2u_2 + (M_1 - M_2)(h_c + KE_c) \tag{2}$$

UNCLASSIFIED
DWG. 21430

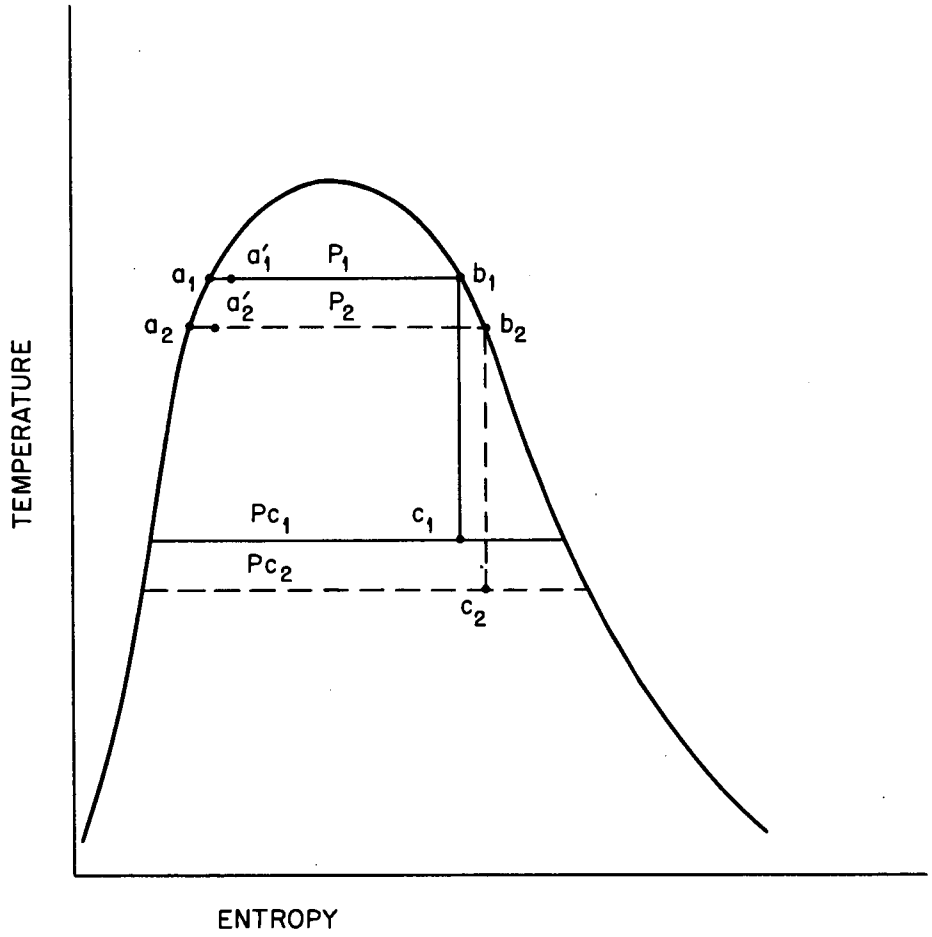

(a)

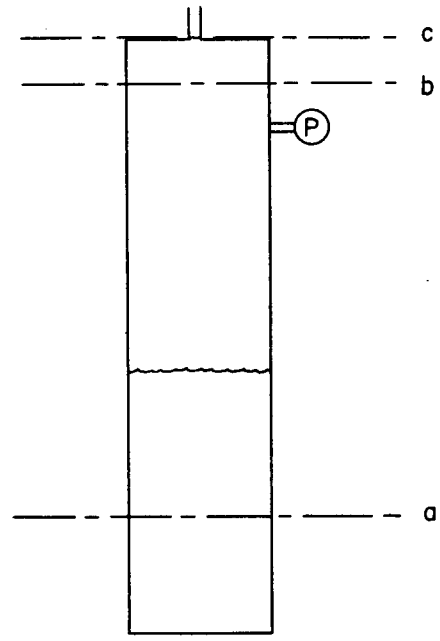

(b)

Fig. 4. Location of Pertinent State Points on T-S Diagram with Corresponding Physical Location in Vessel.

The flow of vapor through the tube is closely approximated over short time intervals by the steady state equation

$$h_b = h_c + KE_c \tag{3}$$

which assumes negligible kinetic energy of the vapor inside the vessel.

When a difference in pressure occurs across the tube the saturated vapor at b_1 expands to point c_1. (See Figure 4.) This expansion is represented by an isentropic line on the diagram. Actually the expansion is not reversible and a velocity coefficient is used to correct this discrepancy. The velocity coefficient is included in the discharge coefficient which will be discussed later. At pressures above about 26 psia, critical flow will occur in the tube. For saturated steam the critical pressure is taken as $P_c = 0.575\ P_1$ (4). This value is technically correct only for a flow nozzle but will be used for the short tube for want of a better value.

As the pressure decreases point b follows the saturation line in Figure 4(a) and point c correspondingly moves downward and to the right. The kinetic energy at point c may be found from equation (3) and the velocity at point c, V_c, may be found from

$$V_c = \sqrt{2g_c\ J\ (h_b - h_c)}, \tag{4}$$

where g_c is the conversion factor in Newton's law of motion and J is the mechanical equivalent of heat. The flow rate is then given by the continuity equation,

$$w_c = \frac{A_c C_D V_c}{v_c}, \tag{5}$$

where w is the flow rate, A is the area of the tube, v is the specific volume of the vapor at point c, and C_D is the coefficient of discharge for the tube. The change in mass, of material in the vessel, is equal to the product of the flow rate and the duration of the time interval, $\Delta\theta$, and is given by

$$\Delta M = M_1 - M_2 = w \Delta \theta. \tag{6}$$

With ΔM and M_2 known, the internal energy of the material in the vessel at time 2 may be found from equation (2).

The specific volume of this material is given by

$$v_2 = \frac{G}{M_2} ,$$

where G is the volume of the vessel.

The two properties, specific volume and internal energy, are sufficient to establish the state of the material in the vessel at the end of the time interval. The pressure, p_2 can then be determined if u_2 and v_2 are known. Once p_2 is found the process may be repeated for the next increment of time.

In the computations made here the Kennan and Keyes steam tables (5) and the included Mollier diagram were very useful. The vapor charts compiled by Ellenwood and Mackey (6) which include enthalpy-specific volume diagrams were helpful in finding the specific volume at point c. To this writer's knowledge there are no published charts including both specific volume and internal energy. To avoid a long trial and error process a chart of pressure vs. quality, with lines of constant internal energy and specific volume, was plotted

using steam table data. The chart is reproduced in Figure 5. The pressure and quality of the material at the end of the time interval are found from the intersection of v_2 and u_2.

Calculations were made for five second intervals for the first thirty seconds and for ten second intervals for the next seventy seconds. The first one hundred seconds after rupture covered the region of interest.

The calculations made for three of the experimental runs are given in tabular form in Tables I, II, and III. The three runs represent two different initial pressures and two different tube diameters. The initial weight of water in all three of these tests was four pounds. The pertinent results from the calculations are tabulated separately for convenience in Tables IV, V, and VI.

Coefficient of Discharge

Flow devices with length to diameter ratios of 1 to 3 and with a uniform cross section are generally called short tubes. Flow through such a device may be of two distinct natures (7). The tube may flow full or may break free from the walls at the entrance and discharge as a sharp edged orifice. This property makes short tubes undesirable as accurate measuring devices and the usual practice is to use a flow nozzle or a sharp edged orifice with a length to diameter ratio not greater than 0.125. This is impractical for a device where the hole size is on the order of 0.0625 in and the pressure drop encountered is very high.

UNCLASSIFIED
DWG. 21431

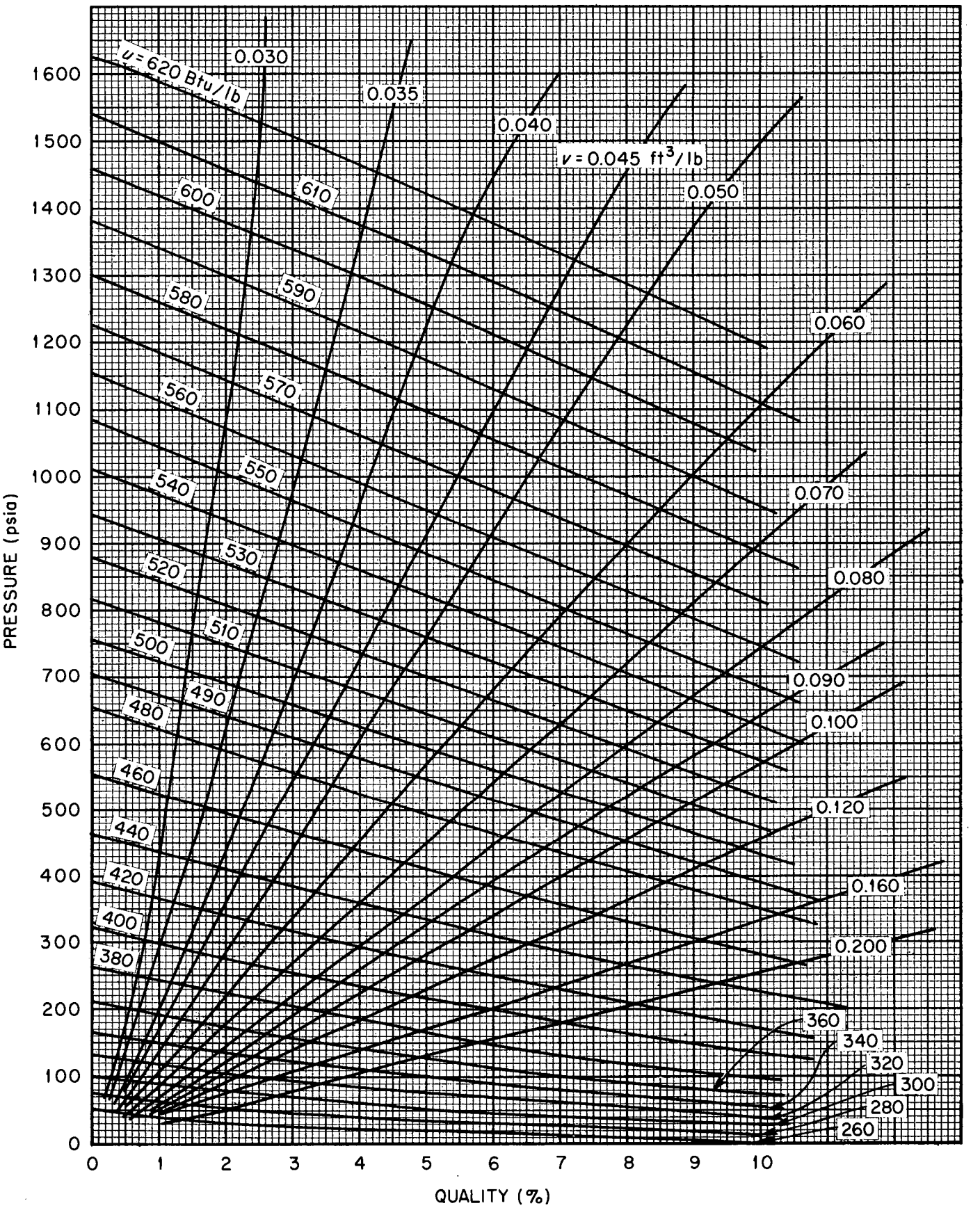

Fig. 5. Pressure vs. Quality Diagram with Lines of Constant Internal Energy and Constant Specific Volume.

TABLE I

TABULATED CALCULATIONS

Initial Pressure - 1540 psia Initial Liquid Weight - 4.00 pounds Restricted Tube Diameter - 0.0625 in

Time Sec	p_1 psia	p_c psia	s_b Btu/deg F	h_b Btu/lb	h_c Btu/lb	v_c ft^3/lb	KE_c Btu/lb	V_c ft/sec	w_c lb/sec	M lb	M_2 lb	v_2 ft^3/lb	u_2 Btu/lb	p_2 psia
0-5	1540	886	1.3307	1165.0	1123.0	0.457	42.0	1450	0.0541	0.2705	3.7295	0.0391	597	1230
5-10	1230	707	1.3600	1182.0	1138.0	0.59	44.0	1484	0.0437	0.2185	3.5110	0.0416	562	987
10-15	987	567	1.3913	1192.0	1147.0	0.76	45.0	1501	0.0337	0.1685	3.3425	0.0437	528	780
15-20	780	449	1.4181	1199.1	1154.5	0.96	44.6	1494	0.0265	0.1325	3.2100	0.0454	502	643
20-25	643	370	1.4385	1202.5	1155.5	1.18	47.0	1533	0.02242	0.1121	3.0979	0.0471	476	538
25-30	538	310	1.4564	1204.0	1157.0	1.42	47.0	1533	0.01840	0.0920	3.0059	0.0486	454	450
30-40	450	259	1.4734	1204.6	1158.5	1.69	46.1	1519	0.01532	0.1532	2.8527	0.0512	412	310
40-50	310	178	1.5075	1203.0	1157.0	2.45	46.1	1519	0.01058	0.1058	2.7469	0.0532	380	230
50-60	230	132	1.5334	1200.0	1154.0	3.27	46.1	1519	0.00793	0.0793	2.6676	0.0547	356	175
60-70	175	100.5	1.5565	1196.4	1151.0	4.25	45.4	1507	0.00603	0.0603	2.6073	0.0560	337	140
70-80	140	80.5	1.5751	1193.0	1148.0	5.25	45.0	1501	0.00487	0.0487	2.5586	0.0570	321	120
80-90	120	69.2	1.5878	1190.4	1146.0	6.0	44.4	1490	0.00423	0.0423	2.5163	0.0580	307	100
90-100	100	57.5	1.6026	1187.2	1143.0	7.2	44.2	1487	0.00352	0.0352	2.4811	0.0588	294	85

TABLE II

TABULATED CALCULATIONS

Initial Pressure - 1540 psia Initial Liquid Weight - 4.00 pounds Restricted Tube Diameter - 0.0625 in

Time Sec	p_1 psia	p_c psia	s_b Btu/deg F	h_b Btu/lb	h_c Btu/lb	v_c ft^3/lb	KE_c Btu/lb	V_c ft/sec	w_c lb/sec	M lb	M_2 lb	v_2 ft^3/lb	u_2 Btu/lb	p_2 psia
0-5	1540	886	1.3307	1165.0	1123.0	0.457	42.0	1450	0.1215	0.6075	3.3925	0.0430	540	850
5-10	850	489	1.4085	1197.1	1150.6	0.895	47.5	1542	0.0661	0.3305	3.0620	0.0477	469	510
10-15	510	294	1.4615	1204.3	1156.3	1.52	48.0	1550	0.0390	0.1950	2.8670	0.0510	418	330
15-20	330	190	1.5019	1203.6	1157.2	2.30	46.4	1523	0.0254	0.1270	2.7400	0.0532	380	230
20-25	230	132	1.5334	1200.1	1154.0	3.25	46.0	1517	0.0179	0.0895	2.6505	0.0552	353	170
25-30	170	98	1.5590	1196.0	1152.0	4.40	44.0	1484	0.0129	0.0645	2.5860	0.0563	333	135
30-35	135	78	1.5781	1192.4	1149.0	5.35	43.4	1574	0.01128	0.0564	2.5296	0.0577	314	110
35-40	110	63.4	1.5948	1188.9	1145.0	6.55	43.9	1482	0.00867	0.0403	2.4862	0.0587	294	93

TABLE III

TABULATED CALCULATIONS

Initial Pressure - 540 psia Initial Weight - 4.00 pounds Restricting Tube Diameter - 0.0625 in

Time Sec	p_1 psia	p_c psia	s_b Btu/deg F	h_b Btu/lb	h_c Btu/lb	v_c ft^3/lb	KE_c Btu/lb	v_c ft/sec	w_c lb/sec	M lb	M_2 lb	v_2 ft^3/lb	u_2 Btu/lb	p_2 psia
0-5	540	310	1.4560	1204.0	1157.0	1.43	47.0	1533	0.0183	0.0915	3.9085	0.0373	488	458
5-10	458	264	1.4717	1204.6	1157.5	1.67	47.1	1535	0.01567	0.0784	3.8301	0.0382	434	390
10-15	390	224	1.4867	1204.4	1156.0	1.95	48.4	1557	0.0136	0.0630	3.7671	0.0388	420	355
15-20	355	204	1.4957	1204.1	1157.0	2.12	47.1	1535	0.01235	0.0618	3.7058	0.0394	408	315
20-25	315	181	1.5060	1203.2	1157.0	2.38	46.0	1517	0.01085	0.0543	3.6515	0.0400	397	280
25-30	280	161	1.5164	1202.3	1156.5	2.68	45.8	1514	0.00965	0.0483	3.6032	0.0405	385	255
30-40	255	147	1.5246	1201.3	1156.0	2.93	45.3	1506	0.00875	0.0875	3.5157	0.0415	366	210
40-50	210	121	1.5412	1199.0	1153.0	3.55	46.0	1517	0.00728	0.0728	3.4429	0.0425	347	164
50-60	164	94.3	1.5620	1195.5	1150.5	4.55	45.0	1501	0.00563	0.0563	3.3866	0.0432	334	144
60-70	144	82.7	1.5728	1193.4	1448.2	5.12	45.2	1504	0.00501	0.0501	3.3365	0.0442	320	124
70-80	124	71.5	1.5851	1190.9	1146.0	5.84	44.9	1499	0.00438	0.0438	3.2927	0.0443	307	108
80-90	108	62.1	1.5963	1188.6	1143.0	6.75	45.6	1510	0.00382	0.0382	3.2545	0.0450	296	92
90-100	92	52.8	1.6094	1185.7	1142.0	7.80	43.7	1478	0.00323	0.0323	3.222	0.0453	288	85

TABLE IV

RESULTS OF CALCULATIONS
Initial pressure - 1540 psia
Initial weight - 4.00 lb
Restricting tube diameter - 0.0625 in

Time Sec	Pressure psia	Flow Rate lb/sec	Heat Release Rate Btu/sec-ft^2
0-5	1540	0.0541	368
5-10	1230	0.0437	322
10-15	987	0.0337	269
15-20	780	0.0265	226
20-25	643	0.0224	199
25-30	538	0.0184	169
30-40	450	0.0153	144
40-50	310	0.0106	104
50-60	230	0.0079	81
60-70	175	0.0060	63
70-80	140	0.0049	53
80-90	120	0.0042	45
90-100	100	0.0035	38

TABLE V

RESULTS OF CALCULATIONS
Initial pressure - 1540 psia
Initial weight - 4.00 lb
Restricting tube diameter - 0.0938 in

Time Sec	Pressure psia	Flow Rate lb/sec	Heat Release Rate Btu/sec-ft^2
0-5	1540	0.1215	758
5-10	850	0.0661	549
10-15	510	0.0390	361
15-20	330	0.0254	250
20-25	230	0.0179	182
25-30	170	0.0129	135
30-35	135	0.0113	121
35-40	110	0.0087	94

TABLE VI

RESULTS OF CALCULATIONS
Initial pressure - 540 psia
Initial weight - 4.00 lb
Restricting tube diameter - 0.0625

Time Sec	Pressure psia	Flow Rate lb/sec	Heat Release Rate Btu/sec-ft^2
0-5	540	0.0183	167
5-10	458	0.0157	148
10-15	390	0.0136	132
15-20	355	0.0124	121
20-25	315	0.0109	107
25-30	280	0.0097	97
30-40	255	0.0088	89
40-50	210	0.0073	75
50-60	164	0.0056	60
60-70	144	0.0050	53
70-80	124	0.0044	47
80-90	108	0.0038	42
90-100	92	0.0032	35

One of the short tubes used in these tests was calibrated with water over the same range of Reynolds numbers encountered in the tests. Based on the 0.0625 in diameter the coefficient varied from 0.775 to 0.812. Examination of the tube under a high powered microscope showed that the hole diameter was slightly larger than 0.0625 in and therefore the discharge coefficient was actually less than 0.8. The hole was drilled in a 0.125 in thick stainless steel plate with a 0.0625 in drill and this made a larger hole than expected. In the calculations a discharge coefficient of 0.8 and a hole diameter of 0.0625 in were used. Based on the results of the calibration of the 0.0625 in tube a coefficient of 0.8 was used for the 0.0938 in tube.

CHAPTER IV

EXPERIMENTAL RESULTS

Analysis of Temperature Data

The complete data from three of the test runs are reproduced from the recorder charts in Figures 6, 7 and 8. The data for each test run are combined on a single graph for ease in comparing the data. The inset diagram shows the location of the thermocouples on the vessel. Two of the runs were made with an initial pressure of 1540 psia, one with a 0.0625 in diameter restricting tube and one with a 0.0938 in diameter restricting tube. The third run was made with an initial pressure of 540 psia and a 0.0625 in diameter restricting tube. The initial weight of water in all three of the test runs was 4.00 lb.

A comparison of the variation in wall temperature with time shows that the lower part of the vessel cools much more rapidly than the upper part of the vessel. Temperatures 1 and 2 near the bottom of the vessel tend to follow the saturation temperature of the liquid in the vessel. Temperatures 3 and 4 decrease less rapidly. The difference in cooling rates is attributed to the difference in heat transfer rates of metal to steam and metal to water.

In the liquid region heat transfer takes place by conduction and boiling off the vessel walls, and high rates of heat transfer are possible. In the vapor region the heat is transferred by conduction and radiation, and if the vapor is wet, by boiling from the walls, and

UNCLASSIFIED
DWG. 21432

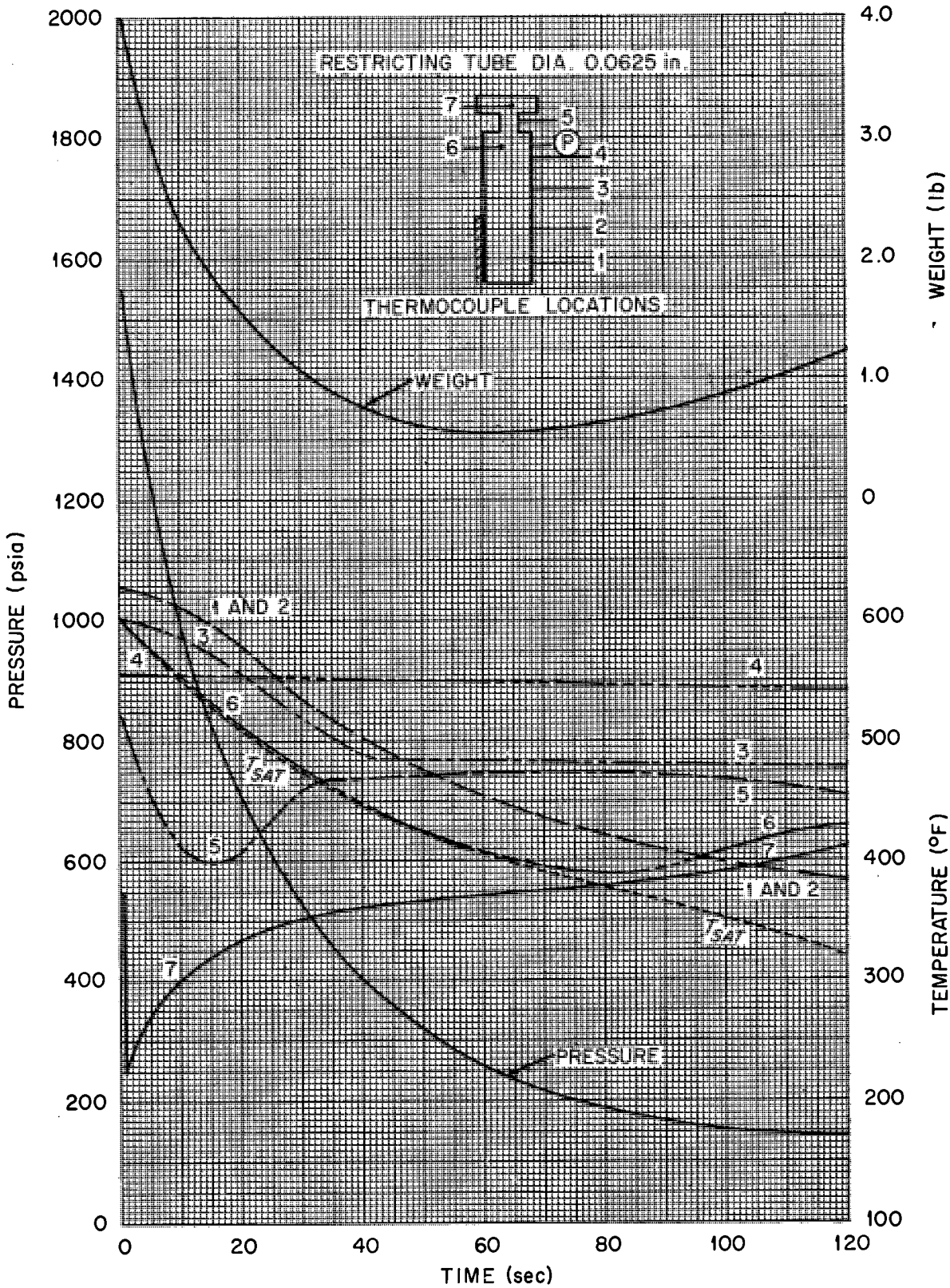

Fig. 6. Complete Test Data from Run 2A.

UNCLASSIFIED
DWG. 21433

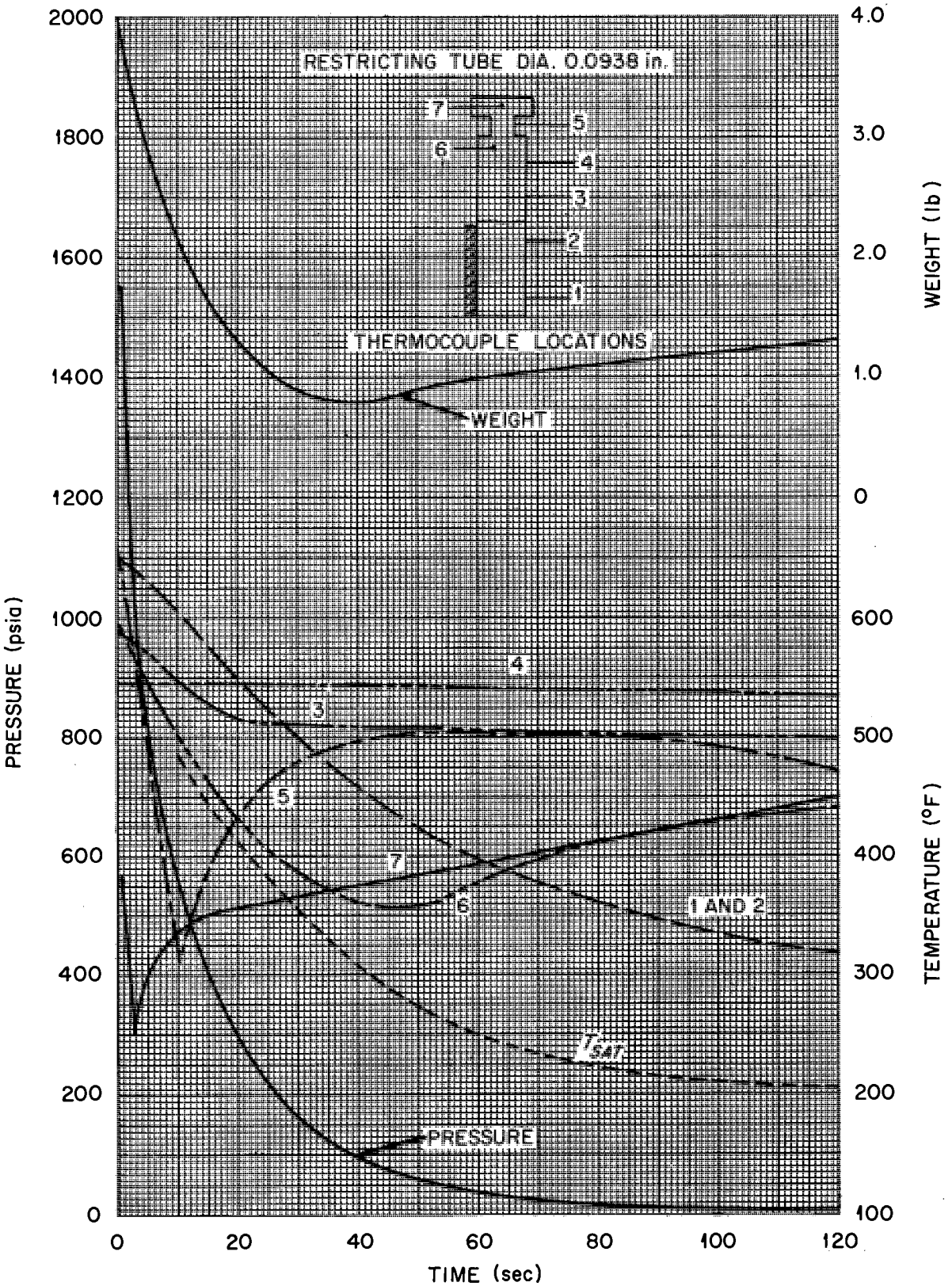

Fig.7. Complete Test Data from Run 1A.

UNCLASSIFIED
DWG. 21434

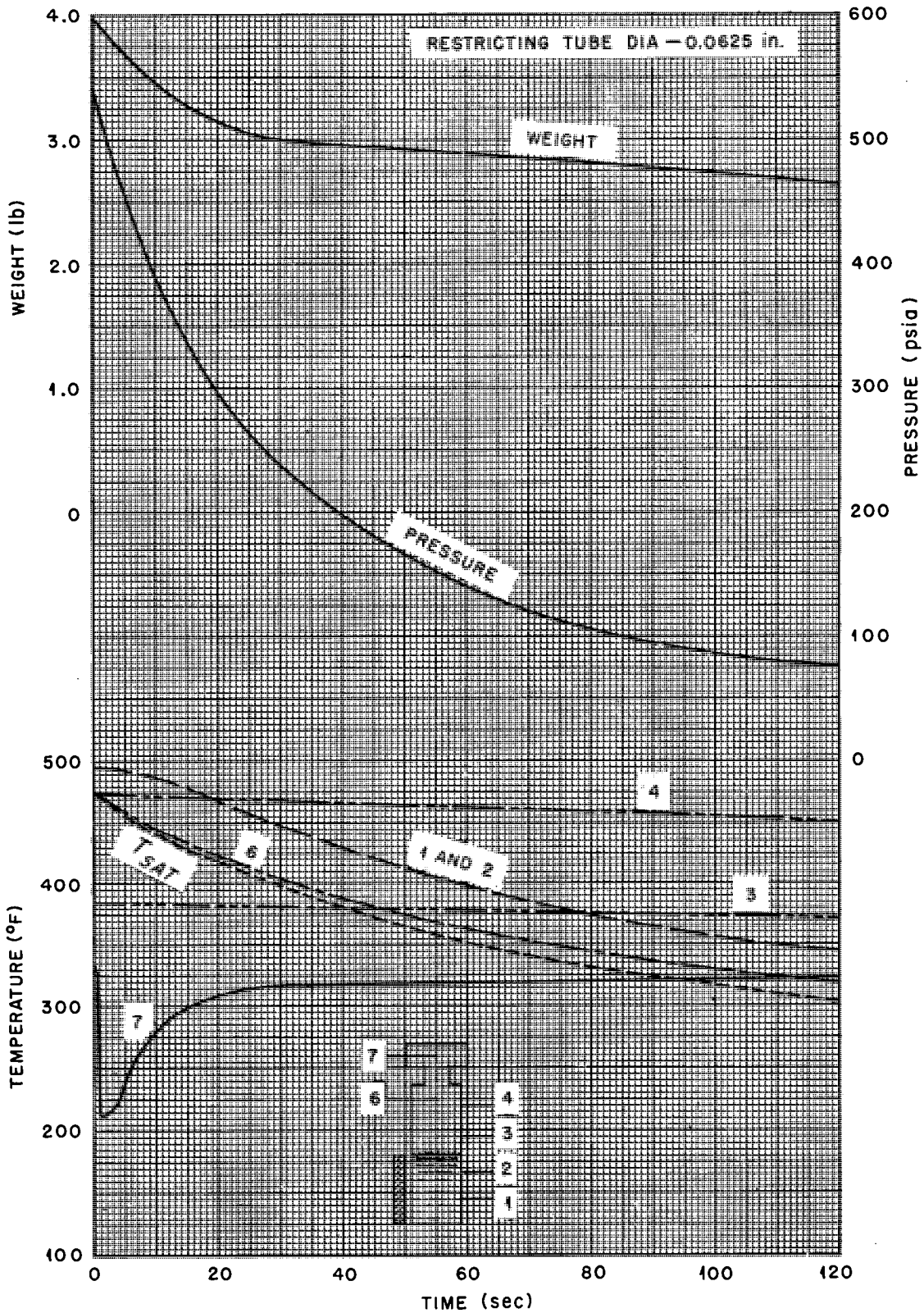

Fig. 8. Complete Test Data from Run 4A.

the heat transfer rate is lower. It appears that the temperature measurements are a good indication of the liquid level in the vessel. In Figure 6 it may be seen that the temperature at point 4 decreases slowly and almost linearly with time indicating no abrupt change in the rate of heat transfer in this location. The temperature at point 3 decreases rapidly for the first forty seconds, and then levels off. This suggests that the boiling level, shortly after rupture, was between points 3 and 4, and after forty seconds was between points 2 and 3. Temperatures 1 and 2 were practically the same during the test runs, indicating that the liquid level never dropped below point 2. The curves of Figure 7 indicate almost the same changes in level. The curves of Figure 8 indicate that the liquid level was below point 3 during all of the run.

In all three of the test runs the comparison of the measured vapor space temperature and the saturation temperature, corresponding to the pressure variation in the vessel, indicates that the vapor is originally saturated, but becomes superheated as the pressure decreases. A heat balance on the upper section of the vessel indicates that most of the heat transferred from the vessel wall is transferred into the contents of the vessel. This heat is available to superheat saturated vapor or to vaporize entrained liquid. For an example, consider the data of Figure 6 at the time when the pressure is 800 psia. Assume the top six inches of the cylindrical vessel wall are at an average temperature indicated by the thermocouple located on the outside of

the vessel at point 4. From the slope of this temperature line and the mass and specific heat of the top six inches of the vessel, the cooling rate was computed to be 0.187 Btu per sec. The heat loss for this section of the vessel through the two inch magnesia insulation was computed to be 0.028 Btu per sec. The heat transferred by conduction down the wall of the vessel to the location of the number 3 thermocouple, based on the difference in temperature between the thermocouple readings, was computed to be 0.016 Btu per sec. The heat transferred upward to the top end plate was neglected, since the end plate was originally at a temperature near that of point 4. The heat entering the fluid is then equal to the wall cooling rate minus the heat transferred down the vessel walls and through the magnesia insulation, and is equal to 0.143 Btu per sec. The calculated flow rate at 800 psia for this test was 0.0265 lb per sec. If this material is dry saturated steam when leaving the liquid surface it will be superheated 11.2 deg. F, taking the specific heat as 0.48 Btu/lb-deg. F. On the other hand if the material leaving the liquid surface contains entrained liquid the heat given up by the walls is sufficient to vaporize 2.08×10^{-4} lb per sec, based on a latent heat of 689 Btu per lb. This indicates that steam leaving the surface at a quality of 99.2 per cent would become saturated steam before leaving the vessel. It is interesting to note that if 0.143 Btu per sec are transferred into the vessel that the heat transfer coefficient from the wall to the vapor based on a fifty degree temperature difference and an area of 0.5 sq ft, is about

20 Btu/hr-ft^2-deg. F. This is somewhat higher than would be expected for heat transfer by convection from the walls to dry vapor, since the vapor velocity is only about 0.2 ft per sec. This relatively high heat transfer coefficient is attributed to droplets of liquid entrained in the vapor being vaporized by contact with the walls.

The above calculations are based on the assumption that the average temperature of the upper six inches of the vessel is given by the thermocouple at point 4, and are therefore not extremely accurate, however they do show the order of magnitude of superheating or vaporizing caused by the vessel walls. As the pressure decreases the flow rate also decreases and there is less tendency for entrainment at the liquid surface and less vaporization occurs as the vapor passes through the top section. With lower flow rates higher superheating occurs due to the greater time of contact between the vapor and the vessel walls. The curves in Figures 6, 7, and 8 indicate that the temperature in the vapor space departs further from the saturation temperature with increasing time.

The measurement of temperature downstream from the restricting tube may be used as an approximate indication of the conditions upstream from the tube if a steady flow equation is used to approximate the unsteady state flow from the vessel. The enthalpy at the downstream thermocouple location is assumed to be the same as the enthalpy before the restricting tube. This assumes that the kinetic energy in the jet is converted to enthalpy in the enlarged section. With these

assumptions, which are admittedly not entirely valid, the thermocouple temperature measurement is used in the same manner as the thermometer in a throttling calorimeter. The pressure and temperature locate the end point of the expansion in the superheat region. With the enthalpy of this state point and the vessel pressure for the corresponding time, the state point of the material upstream from the tube may be determined and the quality of the steam may be found.

The quality can be conveniently determined from a Mollier diagram. Figures 9 and 10 are small sections of a Mollier diagram with this process represented. The points on the atmospheric pressure line are the downstream temperatures. From these points constant enthalpy lines are drawn back to the pressure at the corresponding time and this intersection locates the state of the vapor in the upper section of the vessel. The measured vapor temperature and the saturation temperature are also plotted as a comparison. In Figure 9 the downstream measurement indicates that the vapor in the vessel is wet for the first forty seconds after rupture and indicates higher superheats than the temperature measurement in the vessel after about sixty seconds. Figure 10 indicates that the vapor is dry and saturated for the first seven seconds and that the steam is superheated for the duration of the run. The agreement with this temperature and the vapor space temperature is not very good but they both indicate the same type of trend, i.e., that the vapor becomes superheated as the pressure decreases.

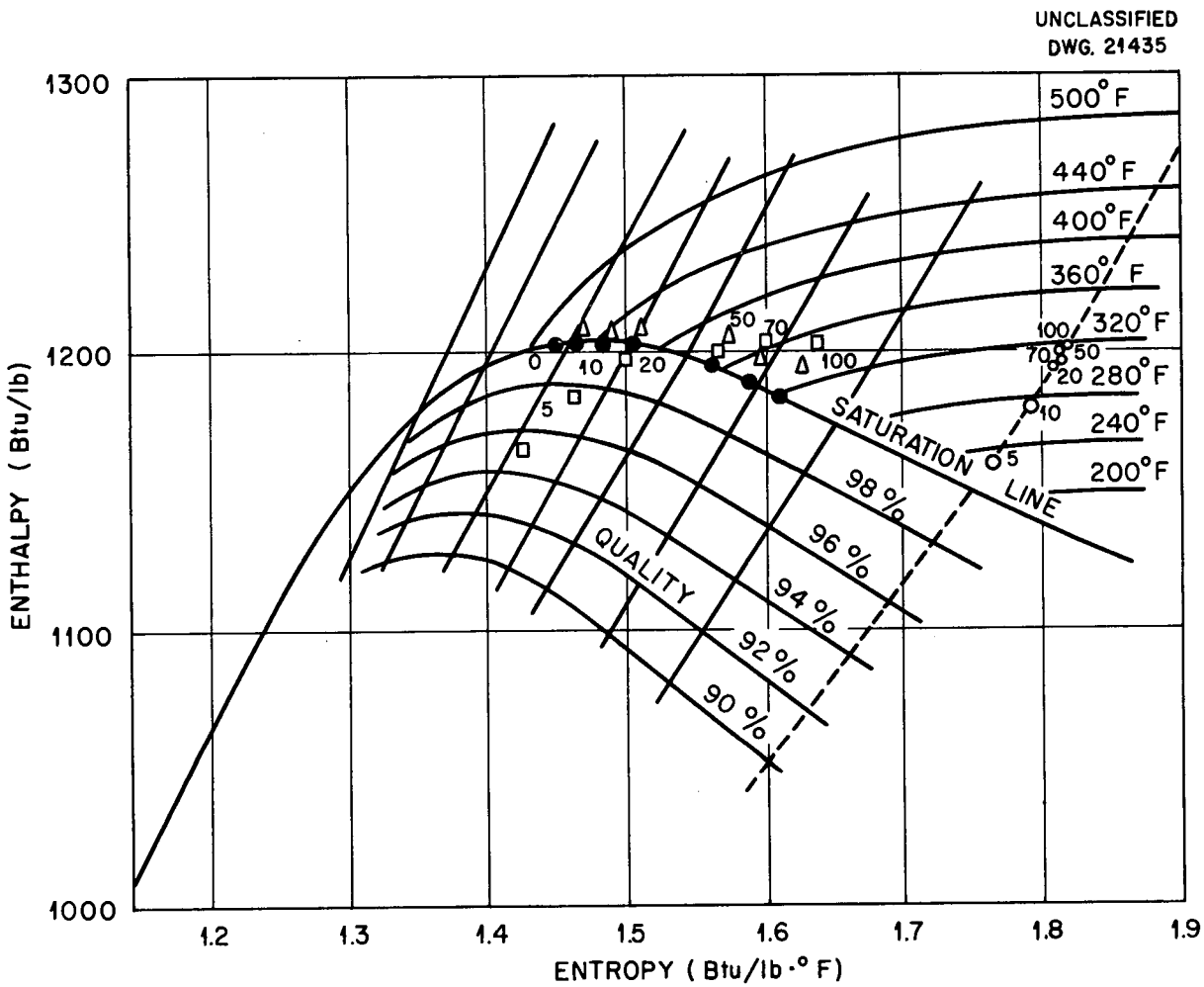

○ DOWNSTREAM TEMPERATURE

Δ VAPOR TEMPERATURE IN VESSEL

□ POINT ASSUMING $h_b = h_d$ (AS IN THROTTLING CALORIMETER)

● POINT ASSUMING SATURATED CONDITIONS IN VESSEL

NUMBERS ARE TIME IN SECONDS AFTER RUPTURE

Fig. 9. Temperature Data from Run 4A Plotted on Mollier Chart.

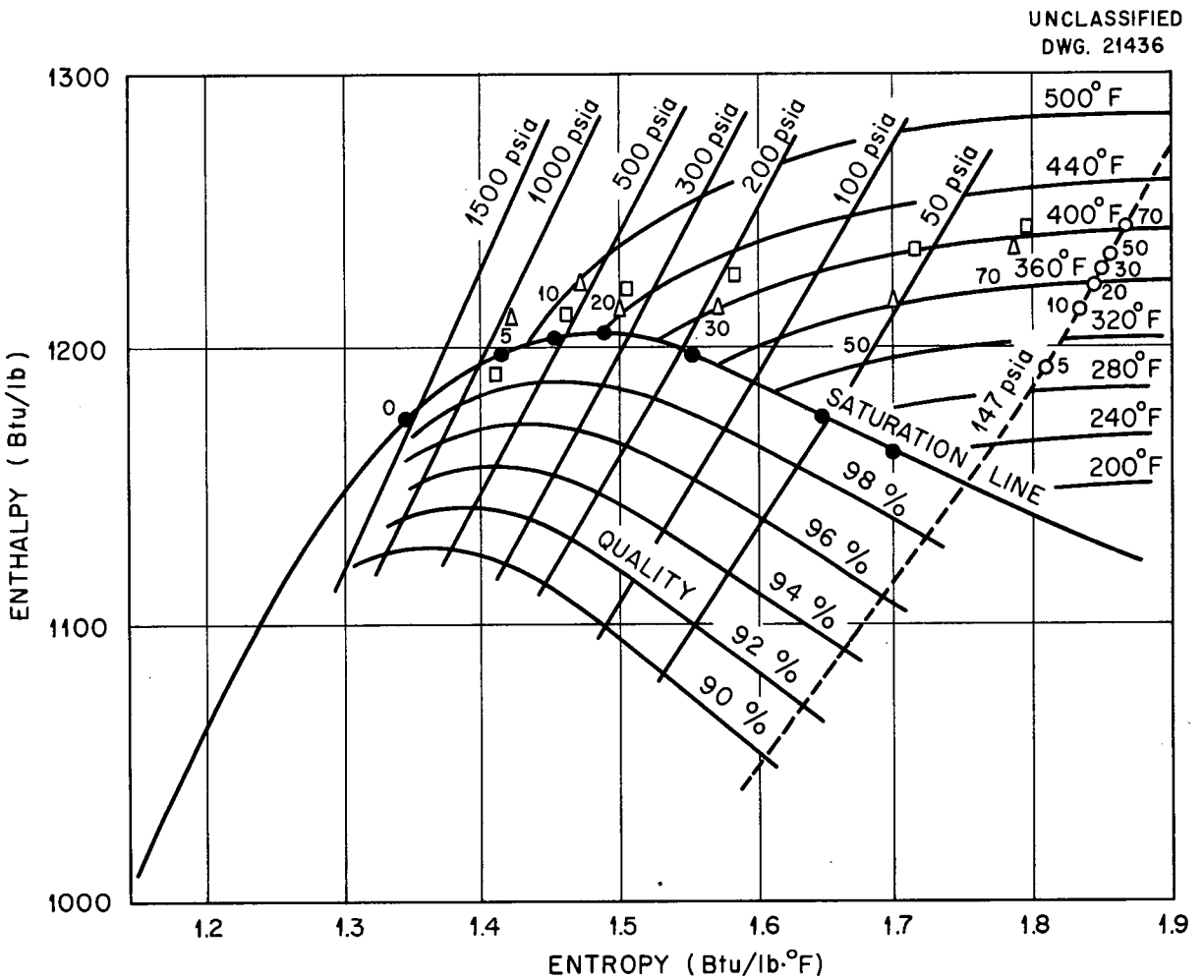

○ DOWNSTREAM TEMPERATURE

Δ VAPOR TEMPERATURE IN VESSEL

□ POINT ASSUMING $h_b = h_d$ (AS IN THROTTLING CALORIMETER)

● POINT ASSUMING SATURATED CONDITIONS IN VESSEL

NUMBERS ARE TIME IN SECONDS AFTER RUPTURE

Fig. 10. Temperature Data from Run 1A Plotted on Mollier Chart.

The temperature measurements mentioned previously indicate that the boiling level was above point 3 during the period following burst in the two runs at the higher pressure. The non-boiling liquid depth for four pounds of water is about nine and one half inches. Point 3 corresponds to a depth of twelve inches. During the time the level was above point 3 the volume fraction of vapor in the boiling liquid was therefore equal to or greater than $1 - \frac{9.5}{12} = 0.21$. Assuming the liquid dropped below point 3 at the time the temperature of this point stopped changing rapidly and leveled off to a gradual decrease, establishes one point where the vapor fraction may be determined as a function of power removal and pressure. From Figure 6 this point occurs at about forty seconds. The pressure at this time was 400 psia and the heat release rate was 144 Btu per sec per sq ft. Heat removal rates for such a system are sometimes quoted as power densities in KW of power removed per liter of boiling liquid. The power density for this point is therefore 4.93 KW per liter at a pressure of 400 psia and a vapor fraction of 0.21. At the similar point in Figure 7 the power density is 6.22 KW per liter at a pressure of 210 psia and a vapor fraction of 0.21. In test run 5A (Figure 8) the boiling level, judged by the temperature measurements, was always below point 3 and on this basis it can be stated that at 450 psia the power density was greater than 5.75 KW per liter with a vapor fraction of less than 0.21.

The above vapor fractions are based on four pounds of liquid in the vessel at the point of interest. They may be corrected by using the liquid level corresponding to the calculated weight at that time as the non-boiling level. The corrected values are tabulated in Table VII.

These values tabulated above do not follow a logical trend. It would be expected that the vapor fraction would have been higher in run 5A based on the values found in runs 2A and 1A. If more thermocouples had been placed on the outside of the vessel more points of the above type could have been obtained.

Pressure Drop Versus Time

The greater the mass of saturated liquid in the vessel at the time of rupture the longer will be the time required for the pressure to decrease to a given value. As the pressure is reduced part of the liquid is vaporized and an increase in specific volume occurs. The increase in volume tends to increase the pressure and as a result the pressure decreases less rapidly than it would for a system containing a fluid entirely in a gaseous phase. Figure 11 shows experimental evidence of this phenomena from three test runs made with different amounts of liquid but with other conditions equal.

In one test run the vessel was almost filled with water and heated very rapidly. As a result the system reached rupture pressure with the water far below saturation temperature. At rupture the pressure decreased to atmospheric pressure in about three sec. The pressure would have decreased less rapidly if the water had been saturated.

TABLE VII

POWER DENSITY ATTAINED WITH CORRESPONDING PRESSURE AND VAPOR FRACTION

Test Run	Pressure (psia)	Power Density (KW/l)	Vapor Fraction
2A	400	4.9	0.47
1A	210	6.2	0.51
5A	450	5.7	0.26

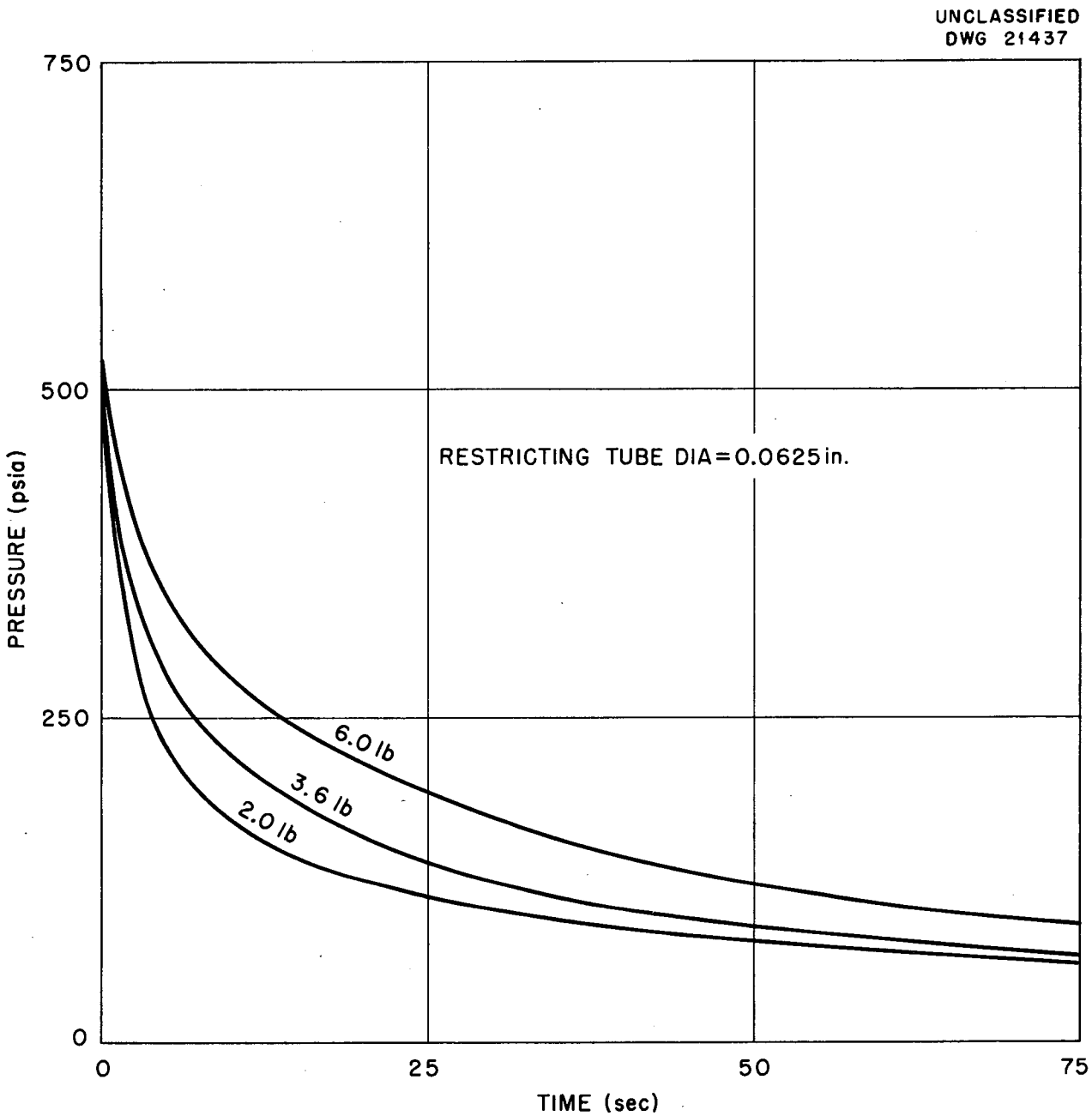

Fig. 11. Variation of Pressure with Time for Various Initial Weights of Liquid.

Figures 12, 13, and 14 show the variation of pressure with time as computed and as measured. The computed pressure curve predicts initially a less rapid and later a more rapid decrease in pressure with time than that measured. The later variation is to be expected since the analytical method assumes no heat transfer into the contents of the vessel. In the actual tests the heat transferred from the vessel walls vaporized liquid and tended to slow down the rate of pressure change. The general agreement between the analytical and measured pressure relations is good for all three of the tests. This is a good indication that the flow rates obtained are reasonably accurate.

Flow Rates

The rate of flow of steam from the vessel was determined in the analytical treatment mentioned before. An approximate check is obtained by again resorting to a steady state flow equation applied to a number of small time increments. Grashof obtained the following expression (8) for flow of saturated steam through a flow nozzle where the downstream pressure was less than 0.575 times the upstream pressure:

$$W = 0.0165\ A_2 P_1^{.97}\ , \qquad (4)$$

where W is the flow rate in lb per sec, A_2 is the nozzle area in sq in, and P_1 is the upstream pressure in psia. In applying this equation to the experiment the area was multiplied by a discharge coefficient 0.8. The upstream pressure was taken from the pressure data as the average

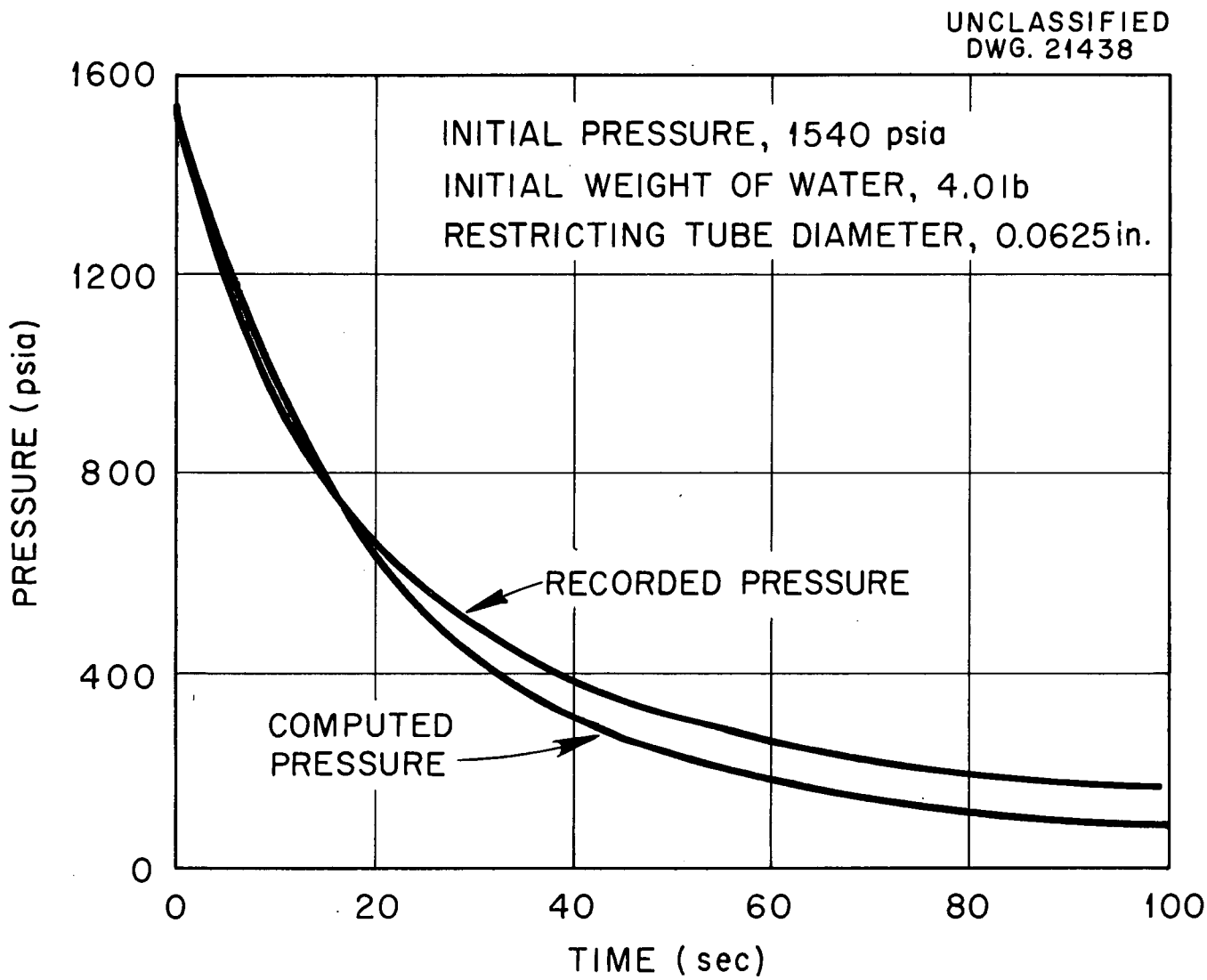

Fig. 12. Variation of Pressure with Time as Computed and as Measured in Run 2A.

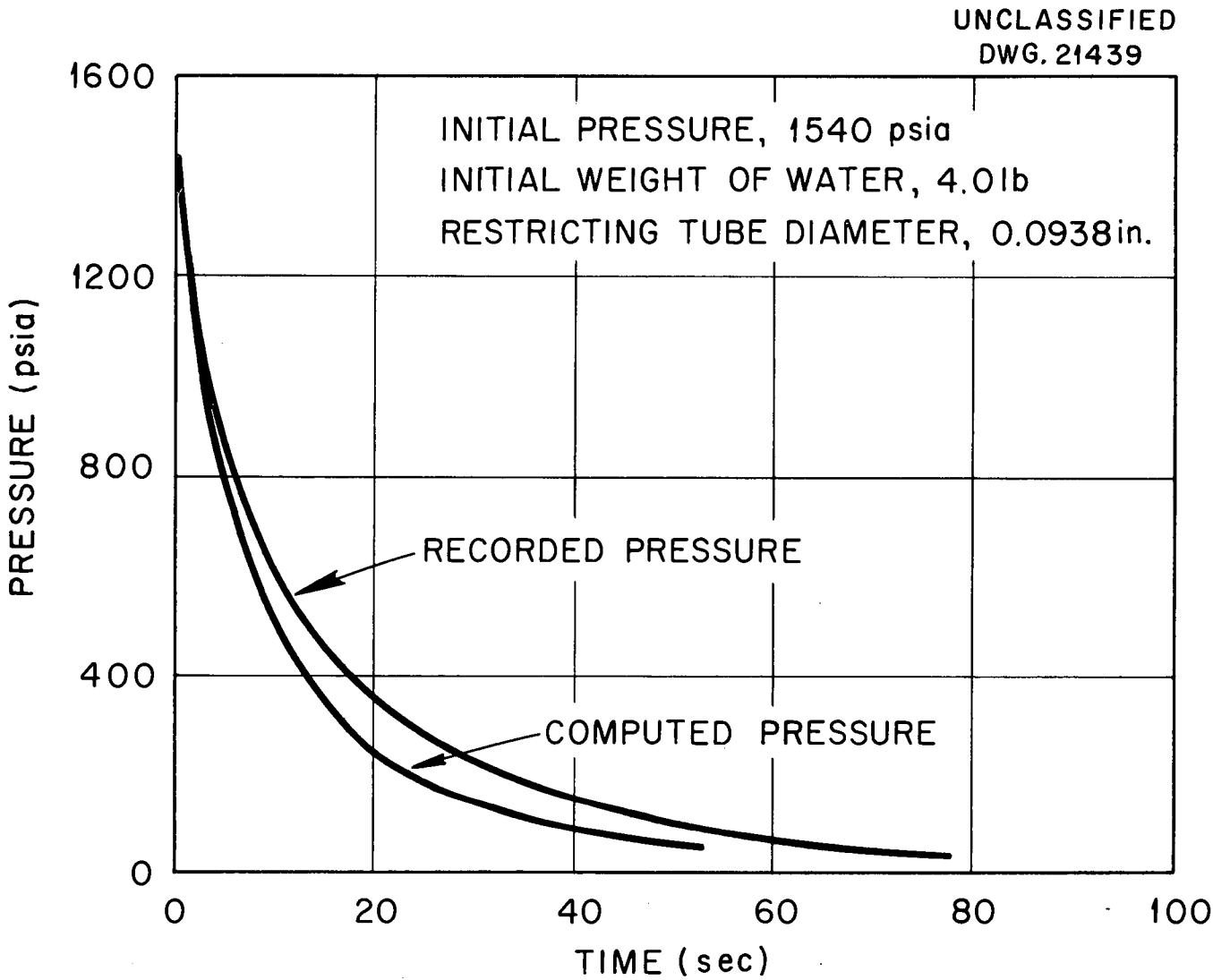

Fig. 13. Variation of Pressure with Time as Computed and as Measured in Run 1A.

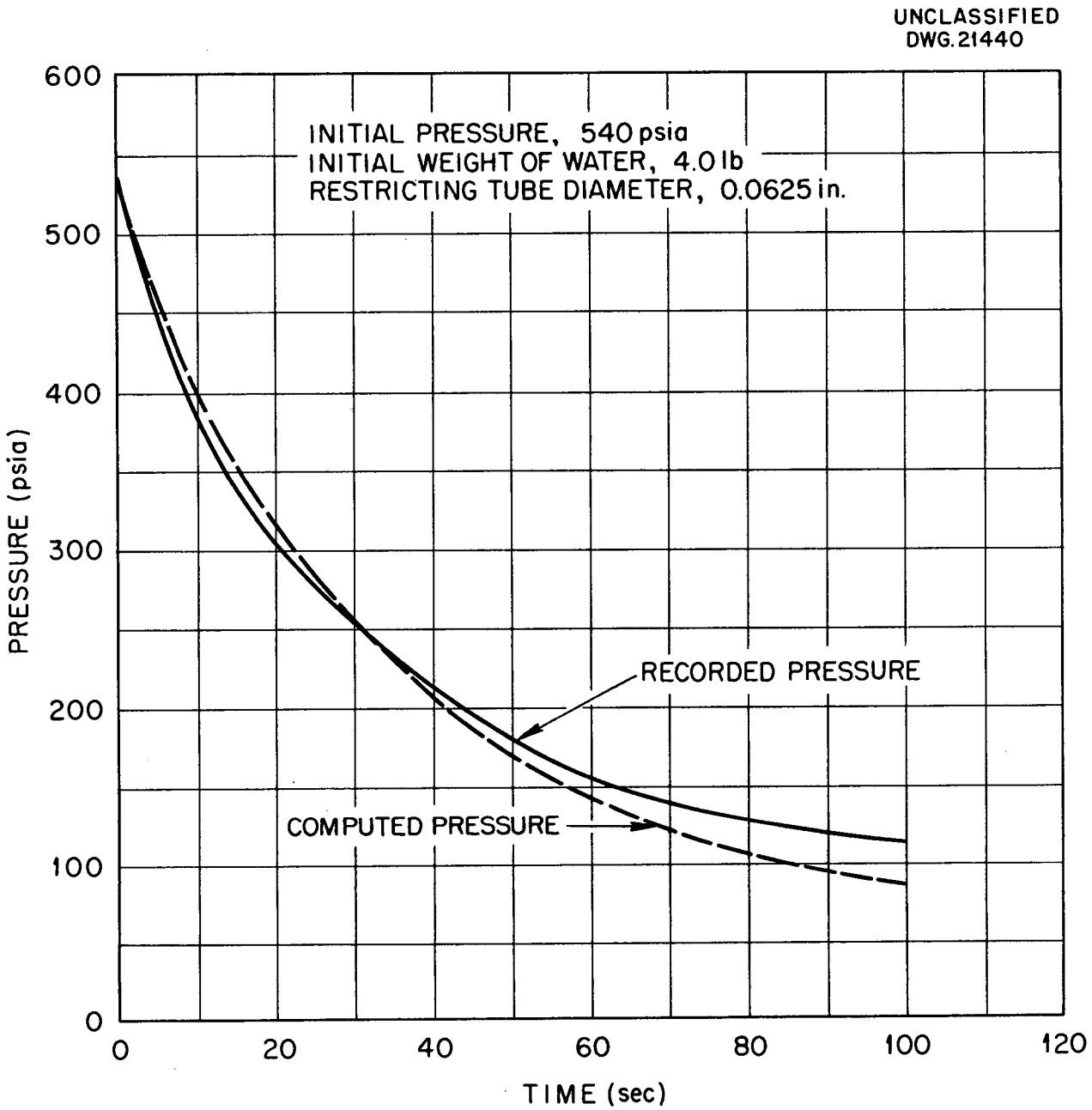

Fig. 14. Variation of Pressure with Time as Computed and as Measured in Run 4A.

pressure over the time increment. The results obtained by applying this equation to one of the test runs are tabulated with the data obtained by the analytical method in Table VIII. The agreement is fair except at the lower pressures where the Grashof equation predicts higher flow rates. In this region the analytical method predicted lower pressures than those measured and this may account for the discrepancy.

The results from the weigh mechanism, had they proved to be reliable, would have been an excellent check on the computed flow rates. However, the data obtained from this instrument were apparently in error. Figures 15(a), 15(b), and 15(c) show the weight of material in the vessel as measured by the weigh beam and as computed by the analytical method. The weight measurements for the two runs at 1540 psia reproduced in Figures 15(a) and 15(b) indicate that the weight decreases more rapidly than predicted by the calculations and then increases gradually until it approaches the calculated weight curve. The 540 psia weight data reproduced in Figure 15(c) does not show the tendency to increase but is always lower than the computed weight. The increase in weight does not appear reasonable and it is suspected that the reading is too low over the region of interest.

It was not possible to get a reliable check on the weight at the end of the run because no means was available to shut off the steam flow at the desired time. The only checks possible were made several hours after the test, when the vessel had cooled down. The amount of liquid was then measured for some of the runs by measuring the liquid

TABLE VIII

COMPARISON OF FLOW RATES OBTAINED USING
GRASHOF EQUATION AND THE ANALYTICAL METHOD
Initial pressure - 1540 psia
Initial weight - 4.00 lb
Restricting tube diameter - 0.0625 in
Pressure data for Grashof equation is from test run 2A (Figure 6)

Time Sec	Analytical Flow Rate lb/sec	Grashof Flow Rate lb/sec
0-5	0.0541	0.0457
5-10	0.0437	0.0350
10-15	0.0337	0.0270
15-20	0.0265	0.0235
20-25	0.0224	0.0207
25-30	0.0184	0.0185
30-40	0.0153	0.0163
40-50	0.0106	0.0125
50-60	0.0079	0.0103
60-70	0.0060	0.0081
70-80	0.0049	0.0072
80-90	0.0042	0.0061
90-100	0.0035	0.0054

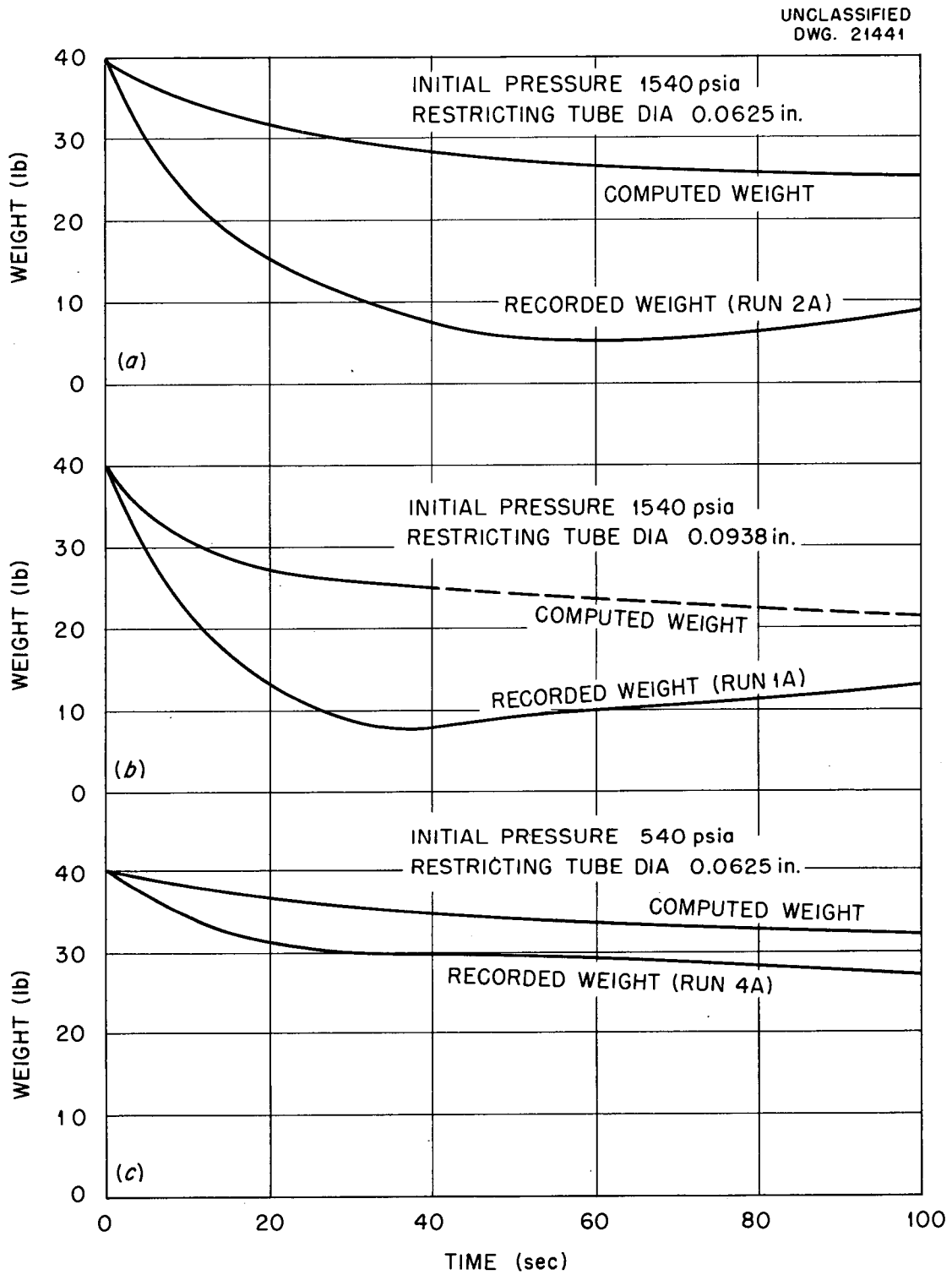

Fig. 15. Variation of Weight of Liquid in Vessel With Time as Computed and Measured in Runs 2A, 1A, and 4A.

level in the vessel with a wooden rod. It was generally found that the amount of water in the vessel at this time was between the end points shown in Figures 15(a), 15(b), and 15(c). The level measured several hours after the test would of course be lower than the level at the end of the test because water was vaporized as the vessel cooled down.

Two different baffle arrangements were placed on the flange opening to force all of the leaving vapor to pass out of the system in a horizontal direction to eliminate any vertical thrust which would effect weight readings. The simplest baffle was merely a twelve inch circular plate which can be seen in Figure 3. There was some question as to the possibility of steam reversing its flow and leaving with a downward velocity component. This would tend to lift the vessel up and cause a lower weight reading during the period of high flow rates. To check this effect an eighteen inch square baffle was placed one inch below the original baffle with a solid section extending down to the opening of the flange. The top baffle was enlarged to the same dimensions as the lower baffle. In this arrangement all of the vapor had to leave the system in a horizontal plane. The same type of results were obtained with either baffle arrangement and it was concluded that there was no appreciable effect on the weight readings caused by thrust due to vapor leaving the system. No reasonable explanation for the apparent weight reading discrepancies has been obtained.

Heat Release Rates

The heat release rates were obtained from the analytical results. The results obtained are tabulated in Tables 4, 5, and 6 with the computed flow rates for the three test runs analyzed. The maximum heat release rate obtained was 758 Btu per sec per sq ft of surface. This was during the five second interval following rupture for the run at an initial pressure of 1540 psia with the larger diameter restricting tube.

CHAPTER V

CONCLUSIONS AND RECOMMENDATIONS

The general agreement between the measured and computed rates of pressure decrease indicates that the analytical treatment used was reliable and that flow rates obtained by this treatment are reasonably accurate.

Based on the computed flow rates the maximum heat release rate obtained was 758 Btu per sec per sq ft. The heat release rates varied throughout the test run and were considerably below this maximum for most of the runs.

Values for the decrease in mean boiling liquid density due to the high heat release rates were obtained from the temperature measurements on the vessel walls. The fraction of vapor in the boiling liquid was greater than 50 per cent by volume for the very high heat release rates. More information on boiling levels could have been obtained if the number of thermocouples on the vessel wall had been increased.

From the temperature measurements it is concluded that over most of the test run liquid was entrained at the surface, but that by the time the vapor had reached the restricting tube the liquid had been vaporized by heat transferred from the vessel walls. No upper limit was established for heat release rates which would result in severe entrainment.

A reasonably clean liquid-vapor interface existed at the boiling level during most of the test. The downstream thermocouple indicated the vapor leaving the surface was initially wet and then became superheated as pressure decreased and as heat was transferred into the rising vapor from the vessel walls. It is difficult to determine how much liquid was being entrained in the vapor.

It is recommended that further tests of this type be made using larger diameter restricting tubes to obtain higher heat release rates. It is also recommended that the diameter of the vessel be increased. With a small diameter vessel the ratio of wall area to surface area is large and the effect of boiling off the walls provide a sizeable contribution to the total heat released. Increasing the size will reduce the wall effect and leave more of a free liquid surface available for vapor removal.

BIBLIOGRAPHY

BIBLIOGRAPHY

(1) Heat Transfer, Volume I, Max Jacob, John Wiley and Sons, Inc., New York, First Edition, 1949, pages 614-657.

(2) Thermodynamics, J. H. Kennan, John Wiley and Sons, Inc., New York, First Edition, 1941, pages 32-34.

(3) The Flow of a Flashing Mixture of Water and Steam Through Pipes, M. W. Benjamin and J. G. Miller, Transactions of the American Society of Mechanical Engineers, October 1942, p.657.

(4) Mechanical Engineer's Handbook, L. S. Marks, McGraw-Hill Book Co., New York City, Fifth Edition, 1951, p.333.

(5) Thermodynamic Properties of Steam, J. H. Kennan and F. G. Keyes, John Wiley and Sons Inc., New York City, First Edition, 1936.

(6) Thermodynamic Charts, F. O. Ellenwood and C. D. Mackey, John Wiley and Sons, Inc., New York City, Second Edition, 1945.

(7) Flow Stability in Small Orifices, R. P. Northrup, unpublished paper presented at American Rocket Society Annual Meeting, December, 1951.

(8) L. S. Marks Op. cit. p.335

APPENDIX

Details of Instrumentation

Pressure

Sensing Element - Baldwin SR-4 pressure cell, Type BS 347
Serial No. 2K777, Capacity 2000 psi
PRCA/D 10

Adaptor - ORNL Transduced calibration adaptor
Model R-902, Serial No. 104

Recorder - Brown Electronik Strip Chart Recorder
Reed Inst. Section No. 2
Model Y 153X12 V(1)-X-6AK
0-1 millivolt chart speed 240 inches/hr.
Pen speed 3 seconds to cross complete chart.

Calibrated with dead weight tester

Weight

Sensing Element - Shevitz microformer Number 1872
Weigh Assembly

Adaptor - Solo constant voltage transformer and calibration circuit (span and zero adjustments)

Recorder - Brown Electronik Strip Chart Recorder
Reed Inst. No. 14
Model Y153 X11V(β)-X-27A1
Range 0-10 millivolts
Chart speed 240 inches/hr.
Pen speed - 3 inches/full scale

Temperature

Sensing Elements - I.C. couples 30 BWG and 24 BWG

Additional Equipment - Conax Pressure Glands

Recorder - Multipoint (12) Brown Electronik Strip Chart Recorder

Model 153 X 65 P2-X-91A

Reed Inst. Section No. 106

Singlepoint Brown Electronik Strip Chart

Reed Inst. Section No. 1

Range 0-400 °C (I.C.) 240 in/hr 3 sec. full scale

Power Supply

Powerstats - 120 volts, 220 volts

Heater - strip heaters (10) 9 inches long

Calrod heater

Insulation - 2 inches magnesia